RESEARCH ARTICLE

Oxygen Insertion in Propylene to Make Propylene Oxide Over a Highly Stable and Efficient Titanium Silicate Catalyst

Ankit Pandey[1,2], Monojit Nandi[1], Gaurav Dwivedi[1], Ajay Singh[2], Samir Kumar Maity[1,3] and Mukesh Kumar Poddar[1,3,*]

[1] CSIR-Indian Institute of Petroleum, Dehradun 248005, India
[2] Department of Chemistry, Uttaranchal University, Dehradun 248007, India
[3] Academy of Scientific and Innovative Research (AcSIR), Ghaziabad 201002, India

Abstract

Propylene oxide (PO) is a crucial intermediate in the chemical industry, serving as a precursor for polyether polyols, propylene glycol, and various polymers. Traditional industrial PO production methods, such as the chlorohydrin and hydroperoxide routes, are hampered by significant environmental concerns and the generation of undesirable by-products. This study explores the direct transformation of propylene to PO using titanium silicate (TS-1) catalyst. The catalyst (TS-1) was synthesized and characterized by BET surface analysis, X-ray diffraction (XRD), scanning and transmission electron microscopy (SEM/TEM), and X-ray photoelectron spectroscopy (XPS). These analyses confirmed the formation of a crystalline MFI-type framework with well-dispersed titanium sites and a uniform, spherical morphology. Catalytic performance was evaluated in a batch reactor under varying conditions of temperature, pressure, hydrogen peroxide, and methanol concentrations. Under varying conditions, a maximum PO selectivity of 99.5% and a PO yield of up to 9% were achieved. The highest selectivity was obtained at lower H2O2 concentration, while the maximum yield required a higher H2O2 loading. The study also demonstrated the catalyst's reusability and stability over multiple cycles, with minimal loss in activity. Side reactions, primarily the formation of propylene glycol and its ethers, were minimized by controlling water and hydrogen peroxide concentrations. The results highlight the advantages of TS-1, including high selectivity, environmental compatibility, and operational stability, making it a promising candidate for sustainable PO synthesis. This work provides valuable insights into the design of advanced heterogeneous catalysts for green chemical processes and addresses key challenges in the direct transformation of propylene oxide from propylene and hydrogen peroxide.

Keywords: propylene, propylene oxide, TS-1, epoxidation.

Submitted: 29 August 2025
Accepted: 15 September 2025
Published: 08 December 2025

Vol. 2, **No.** 1, 2026.
10.62762/JCERF.2025.147821

***Corresponding author:**
✉ Mukesh Kumar Poddar
mkpoddar@iip.res.in

Citation
Pandey, A., Nandi, M., Dwivedi, G., Singh, A., Maity, S. K., & Poddar, M. K. (2025). Oxygen Insertion in Propylene to Make Propylene Oxide Over a Highly Stable and Efficient Titanium Silicate Catalyst. *Journal of Chemical Engineering and Renewable Fuels*, 2(1), 13–22.

© 2025 by the Authors. Published by Institute of Central Computation and Knowledge. This is an open access article under the CC BY license (https://creativecommons.org/licenses/by/4.0/).

1 Introduction

Propylene oxide is a vital chemical for the polymer industry with a global production capacity of 7 MMT per annum, with an annual growth rate of approximately 5.9% during the years 2019-2024 [1, 2]. USA, China, European, and Asian countries are among those countries that import Propylene oxide (PO) in large quantities. PO is a low boiling point (34 °C) compound and, it is a highly volatile colorless liquid with an odor resembling sweet ether. PO is used as the precursor for the production of various industrially used materials such as polyether polyols, propylene glycol, polyurethane foams, and in the automobile and housing industries [2, 3]. Propylene glycol is mainly used in food additives, cosmetics, and heat-transfer fluids [1]. Lyondell Basell Company uses PO to make butanediol, which is used to make high-performance polymers, solvents, and fine chemicals [4].

Currently, there are two main commercial methods for the production of PO - Chlorohydrin and Halcon methods. Both these methods include two reaction stages with the production of many by-products [5–7]. The chlorohydrin process is the oldest traditional method that produces a large amount of chlorine and salts with lots of wastewater. It requires an expensive oxidant and gives rise to extreme problems of environmental pollution and equipment corrosion [8, 9]. Auto oxidation of ethylbenzene or isobutane is used to produce alkyl hydroperoxide, which acts as an oxidant for catalytic conversion of propylene into propylene oxide with a large amount of co-products. This process requires excessive use of peroxide, and hence requires a high capital investment [7, 8]. It is reported that epoxidation of propylene into propylene oxide involves allylic C-H bond transfer [8–10]. Epoxidation of propylene via a heterogeneous catalyst in the gas phase is one of the most inexpensive processes, and an abundant oxidant like molecular oxygen would be a more environmentally friendly and potentially economically feasible process for PO production [2, 11, 12]. Production of only water as the byproduct makes direct epoxidation of propylene with H_2O_2 [13–15].

The titanium silicate catalyst (TS-1) has been widely utilized in the production of propylene oxide. Numerous investigations have focused on modifying the TS-1 catalyst, such as enhancing its hydrophobic properties and incorporating different metals [16–21]. These alterations have led to increased selectivity for epoxide formation, while largely maintaining the catalyst's overall activity. TS-1 is particularly effective in the selective oxidation with a wide range of organic substrates using 30% aqueous H_2O_2, with notable efficiency in the epoxidation of light olefins [22]. It was also reported that TS-1 catalyst is very active for epoxidation of light olefin in presence of aqueous H_2O_2.

The tetrahedral titanium, which is highly active in epoxidation reactions, is in the silica matrix in a highly dispersed state [3]. The meso and macro pores are precisely controlled and propylene affinity is increased by giving sufficient hydrophobic properties [23, 24].

Converting propylene directly to propylene oxide (PO) through selective oxidation is often considered a significant breakthrough of catalysis [25]. One of the major challenges in this process is the presence of reactive allylic hydrogen atoms, which can lead to unwanted combustion via C-H bond cleavage [26]. Haruta et al. [29] demonstrated that gold nanoparticles, sized between 2–4 nm and supported on titania, can selectively oxidize propylene to PO using a combination of O_2 and H_2 [27]. While this method achieves high selectivity, it is limited by the expensive and unproductive of hydrogen, and the outcome is highly sensitive to the size and structure of the gold particles [28, 29]. Therefore, till date, no catalyst has been reported that enables the industrial-scale production of PO directly from propylene using only environmentally friendly molecular oxygen [8].

Shigeru Sugiyama et al. [11] explored the gas-phase epoxidation of propylene to produce PO using various catalytic materials [10]. Their study reported the use of MCM41 altered with titanium and/or aluminum as a catalyst, which resulted in a PO yield of less than 0.1%. Given these limitations, there is a need for a new approach in selecting both active catalytic species and suitable supports [16]. From this perspective, the study focused on two widely researched and supported catalyst systems TS-1 [17–19] and noble metal-impregnated ZSM-5 [20, 21]. TS-1 is a molecular sieve with an MFI structure, having structural similarities to ZSM-5, where a small number of silicon atoms in the framework are replaced by titanium.

2 Experiment Section

2.1 Chemicals

Tetra Propylammonium Hydroxide (TPAOH), Tetra Ethyl Titanate (TET), and Tetraethyl Silicate (TES) were purchased form sigma Aldrich. Sodium

Carbonate (Na_2CO_3), Hydrogen peroxide (30% w/v in water), and methanol were supplied by Thermo fisher Chemicals. Propylene and Ar gas were purchased from M/s Sigma gases. Distilled Water was prepared in lab.

2.2 Synthesis of TS-1

Titanium Silicate (TS-1) was prepared as method mentioned in the published journal [30]. A solution of the required amount of Tetraethyl titanate (TET) and Tetraethyl silicate was prepared in distilled water. This solution was added with constant stirring in 100 mL of template Tetra propylammonium hydroxide (TPAOH, 25% aq. solution). Then, the mixture was stirred at 50 °C for more than 1 h until the solution became completely transparent. The mixture was poured into a 100 mL PTFE fitted stainless steel (SS) autoclave and kept for more than 72 h with heating at a temperature of more than 150 °C, under autogenous pressure, without stirring. The obtained material was then cooled, filtered, and washed with deionized water. Synthesis material was dried and calcinated at 550oC for 6h.

2.3 Catalyst Characterization

Surface area of fresh and spent catalysts was obtained by N_2 adsorption isotherms at 77K using a Micromeritics ASAP 2020 analyzer, applying the BET method. The surface area (SA) was derived from adsorption data within the relative pressure (P/P_0) range of 0 to 0.35, while the total pore volume (PV) was evaluated at $P/P_0 = 0.99$. For BET analysis, samples underwent degassing at 350°C for duration of 3 hours [31]. The specific surface area and pore volume were determined using the BET and BJH techniques, respectively. Additionally, surface area evaluation was carried out using the t-plot method. Structural characterization was performed using powder X-ray diffraction (XRD) Bruker D8 Advance diffractometer, employing Cu Kα radiation source with wavelength (λ) of 1.5406 Å and a graphite monochromator [32, 33]. The diffraction scans were recorded over a 2θ range of 5°-80°, with a step size of 0.5 degrees (2θ)/min, a step time of 4 seconds, and operating conditions set at 40 kV and 40 mA. The surface morphology was examined using a SEM, specifically the FEI Quanta 200 F model, utilizing a lanthanum hexaboride (LaB_6) filament as the X-ray source. Imaging was carried out in high vacuum (7.0 Pa at the filament) using an Everhart-Thornley Detector (ETD), under secondary electron mode, at accelerating voltages of either 10 or 30 kV [34, 35]. Elemental analysis (EA) was recorded through Energy-Dispersive X-ray Spectroscopy (EDX). High-Resolution Transmission Electron Microscopy (HR-TEM) was conducted with a JEOL JEM 2100 microscope operating at 200 kV and offering a nominal resolution of 0.25 nm. The samples for TEM were prepared by dispersing the powered catalyst in an alcohol-based suspension. X-ray Photoelectron Spectroscopy (XPS) was performed using a Kratos Axis Ultra instrument, equipped with a monochromatic Al Kα X-ray source (hv = 1486.71 eV) and a hemispherical analyzer operating at a pass energy of 20 eV. All measurements were carried out at room temperature under ultra-high vacuum (pressure below 5×10^{-10} Torr). Calibration of the spectrometer was done using the Au $4f_{7/2}$ peak, referenced at 84.0 eV. Sample was affixed to a conductive carbon tape placed over a copper holder and transferred into the chamber. Any charging effects were corrected by referencing the C 1s signal from surface contaminants at 284.8 $\pm$ 0.1 eV [36–38].

2.4 Chemical Analysis

After completing the reaction, the liquid phase was separated from the used catalyst via centrifugation and then transferred into glass vials with 0.22 micron syringe filter, for HPLC analysis. The HPLC measurements were conducted using an Agilent 1260 Infinity II system equipped with a refractive index detector (RID). The separation was performed on a HPX-87H (AMINEX) column (300 × 7.8 mm), paired with a guard column (20 × 4.6 mm, 5 μm), using 5 mM sulfuric acid (H_2SO_4) as the mobile phase. The volume of 10 muL of the sample was injected, with a total run time of 40 minutes. The mobile phase flow rate was maintained at 0.5 mL/min, the column temperature was set to 60°C and the RID temperature was maintained at 50°C. The Hydrogen peroxide concentration utilized in the reaction was also verified prior to each experiment through Iodometric titration, employing a cerium (IV) sulfate solution and Ferroin as the indicator.

2.5 Catalytic Activity: Epoxidation of Propylene

The experimental reaction was conducted in a stainless-steel batch-type autoclave reactor (Parr Model 4597) with a 50 mL capacity (Schemetic diagram in Figure 1). The reactor featured mechanical stirring and a PID controller to regulate the heating system surrounding the vessel. The reaction mixture having 34 mL of methanol, 1 g of hydrogen peroxide, and 0.2 g of the catalyst. After the reaction, residual hydrogen peroxide in the liquid phase was quantified via Iodometric titration, and this value

was used to determine the extent of H_2O_2 conversion. Post-reaction, liquid samples were centrifuged and filter with 0.22 micron syringe filter, to remove the catalyst and collected in glass vials for HPLC analysis, while the gaseous products were captured in a Tedlar bag and analyzed using a refinery gas analyzer (RGA), just to check the product gases. We have studied in a wide range of reaction conditions like temperature variation of 40 -70 ℃, methanol variation of 10- 34ml and H_2O_2 variation of 1 -10g. We have mainly studied the effect of variation of inert gas (Ar), 5 -15 bar in reactant gas propylene (5 and 10 bar). The details product data has been elaborated below in Figures 7, 8 and 9.

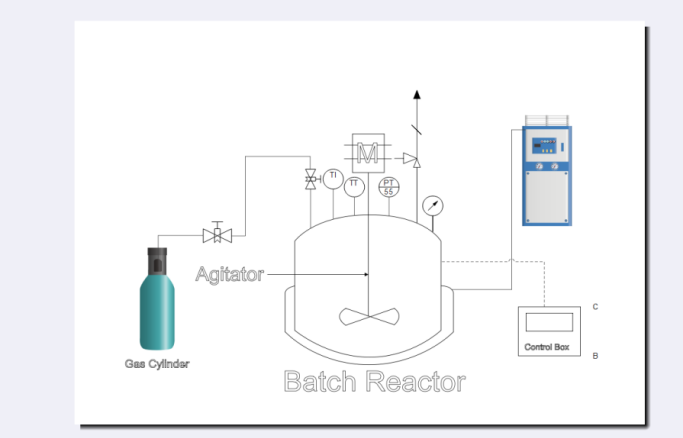

Figure 1. Schematic diagram of batch reactor.

Since the epoxidation of propylene is a rapid and exothermic process, maintaining a stable temperature, especially during the initial stages, presents a challenge. To ensure thermal control, the reactor was equipped with a water jacket to circulate coolant at a consistent temperature. The system included a magnetically driven stirrer, thermocouple, and liquid inlet. The internal temperature was held within ±0.2℃ by dissipating excess heat with chilled water maintained at 13℃. Propylene gas was introduced through a setup consisting of a solenoid valve, mass flow meter, and control valve. Before starting the reaction, the reactor was purged with Argon gas to remove air. Typically, 1 to 4g of aqueous hydrogen peroxide (30wt %), 34g of MeOH, and 0.2g of catalyst were loaded into the reactor. The reaction mixture slurry was heated to the desired temperature range (40–70℃) and subjected to propylene (or a propylene-inert gas mix) at pressures between 5 and 15 bar under stirring about 1h of reaction vigorous agitation. Upon completion, the system was cooled, and products were collected for analysis.

For catalyst stability studies, reusability tests were conducted by recovering the catalyst from previous runs through centrifugation. It was washed with a small amount of methanol and water at ambient temperature and reused after drying. Product selectivity and yield calculations were based on the initial hydrogen peroxide content. Iodometric titration was used to determine both initial and final H_2O_2 levels.

The primary reaction product was propylene oxide (PO), while propylene glycol monomethyl ethers (MME) and propylene glycol (PG) were observed as byproducts. Identification and quantification of the products were performed using High-Performance Liquid Chromatography (HPLC) the detail method is mentioned earlier.

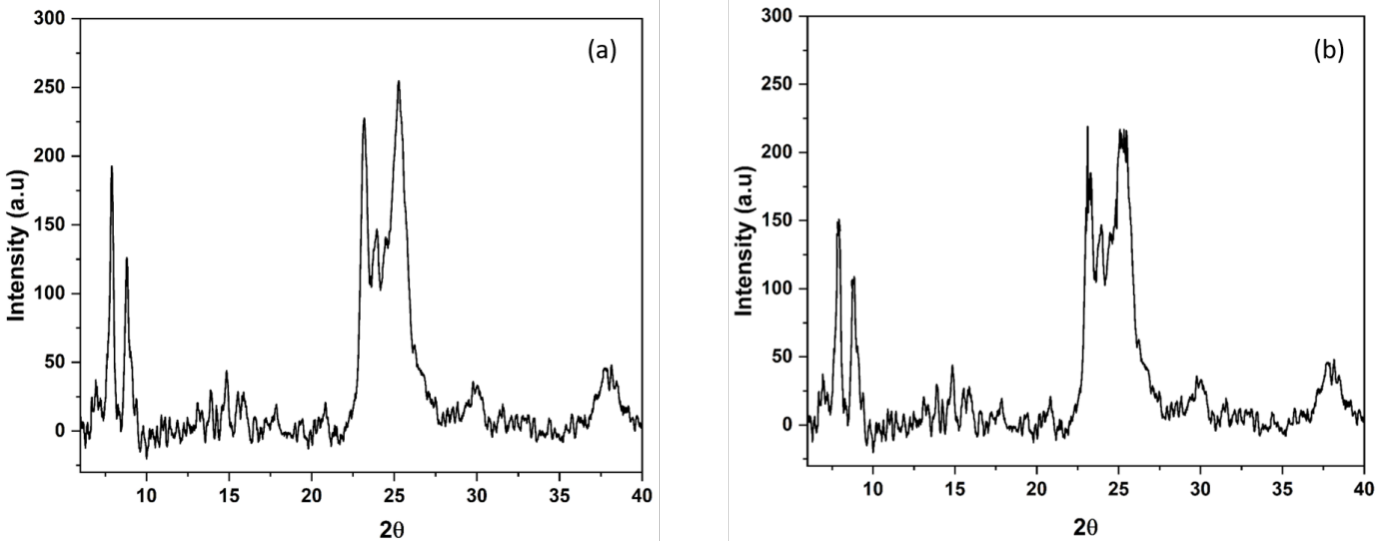

Figure 2. P-XRD diffractograms of catalyst TS-1 (a) fresh, and (b) Spent.

3 Results and Discussion

3.1 Catalyst Characterization

Figure 2 represents the XRD patterns of fresh and spent titanium silicate (TS-1) catalyst. the characteristic diffraction peaks at 2θ values of 7.9°, 8.7°, 23.1°, and 25.3°confirming the presence of the MFI-topology. This catalyst exhibited a higher relative crystallinity (RC), indicating increased alkalinity in the material [32]. The sharp and well-defined peaks in the XRD profile further confirm the crystalline nature of the TS-1 material. The spent catalyst shows slightly less intensity than fresh catalyst at 2θ values of 7.8°, 8.7°, 23.2°, and 25.1°, might be due to slight distortion in crystallinity [33].

Figures 3 and 4 display the SEM and TEM images, respectively, of the synthesized catalyst. The SEM images reveal that the TS-1 sample exhibits predominantly spherical particle morphology with minimal particle agglomeration (Figure 3(a–c)) [34]. In some cases, the formation of irregular or bulk particles may occur, which can be attributed to an insufficient presence of hydroxide ions (OH^-) during the sol-gel synthesis process only [35]. The colloidal sol–gel approach typically leads to the formation of larger structures composed of aggregated nanoparticles, which may be either condensed or exhibit porous, polycrystalline characteristics [36, 37].

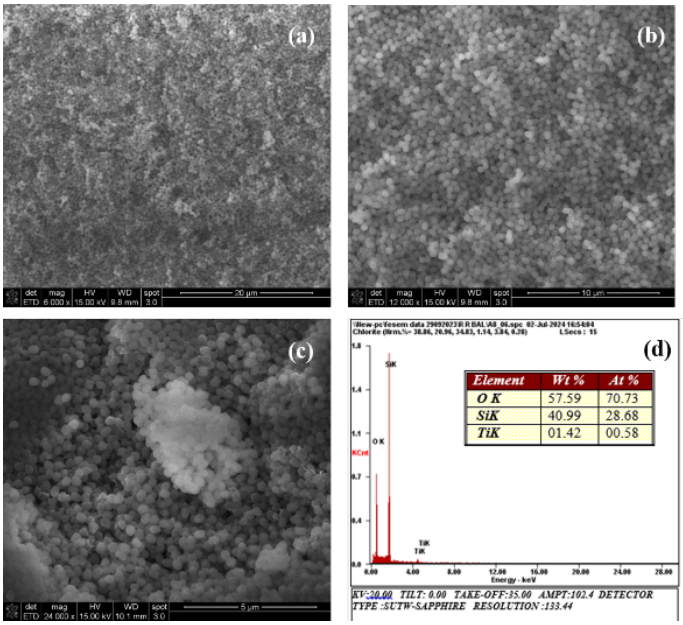

Figure 3. SEM images and EDX plot of catalyst TS-1.

The TEM image presented in Figure 4 reveals clearly defined lattice fringes of the MFI framework in TS-1, reflecting its high degree of crystallinity. This observation confirms the presence of uniformly distributed micropores with an approximate size of 0.5 nm in the TS-1 catalyst [38].

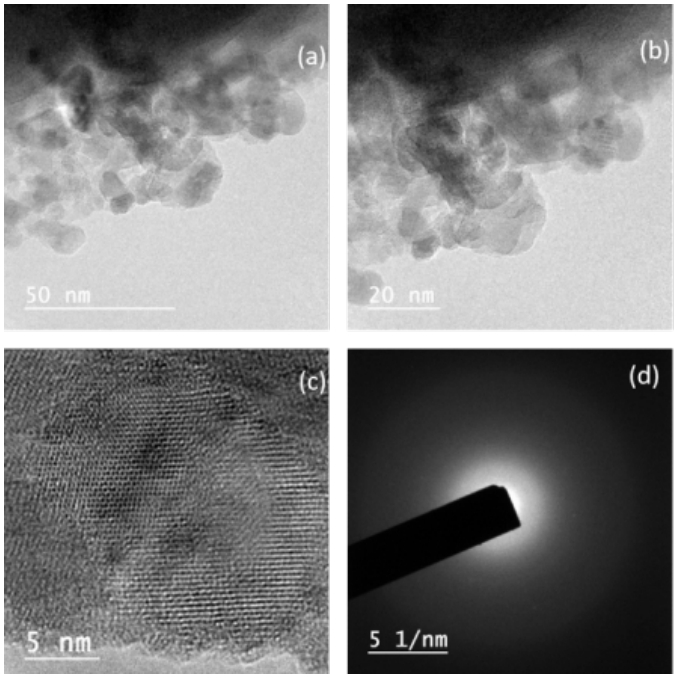

Figure 4. High resolution TEM images of TS-1 (a, b, and c) and SAED pattern (d).

Figure 5 displays the nitrogen adsorption–desorption isotherms for the fresh and spent catalyst. Fresh catalyst (Figure 5(a)) having surface area of 400 m^2g^{-1}, with microporous volume of 0.130 cm^3g^{-1} and External surface area of 87.91 m^2g^{-1}. However spent catalyst (Figure 5(b)) shows surface area of 393 m^2g^{-1} with microporous volume of 0.111 cm^3g^{-1} and External surface area of 126.89 m^2g^{-1}. Result shows that spent catalyst has comparatively less SA and large micropore volume might be due to majority of channels/Ti active site of TS-1 get blocked by organic macromolecules [39–41].

X-ray photoelectron spectroscopy (XPS) was employed to investigate the electronic cloud density around the Ti 2p center, as well as the surface atomic composition, oxidation states, and chemical environments of TS-1 (Figure 6(a): fresh; Figure 6(b): spent). The binding energy associated with tetrahedrally coordinated titanium is observed around 459.86eV for fresh, and 460.07eV for spent catalyst. Whereas octahedrally coordinated titanium exhibits a binding energy at 459.17eV (fresh) and at 459.31 (spent). Shifts in the Ti-2p signal can indicate the formation of Ti–O–Si linkages, which constitute the fingerprint of the titanium in TS-1 [42]. Ti (2p) is slightly higher than that of Ti in pure TiO_2 458.7eV because of the influence

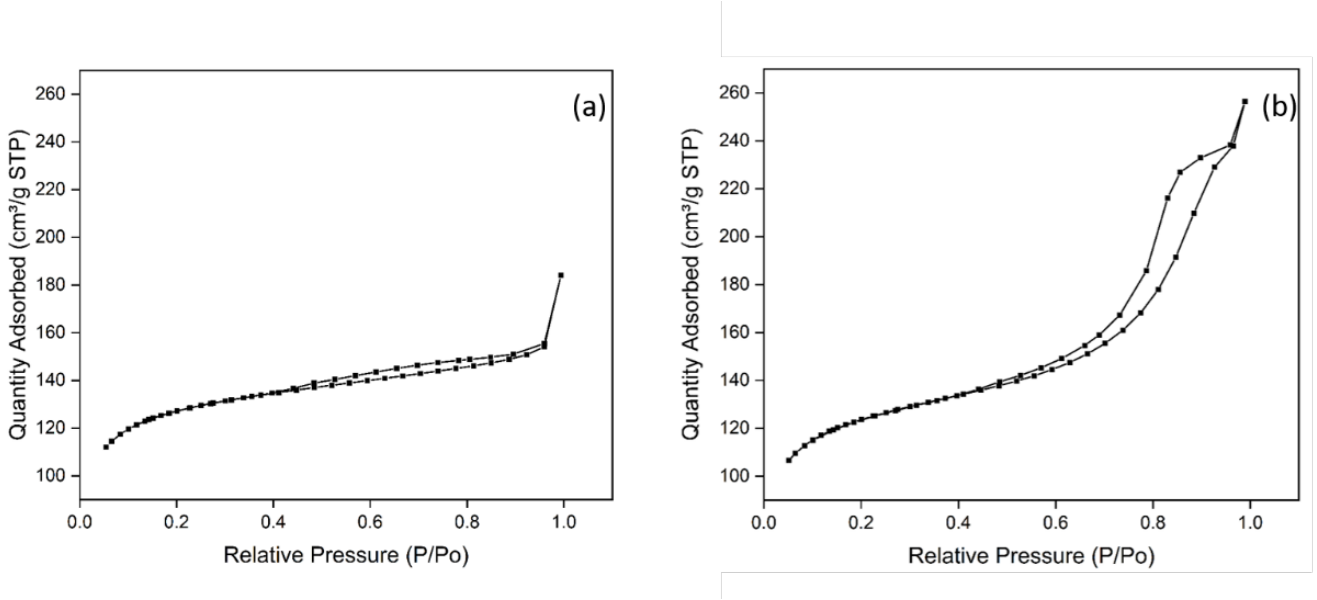

Figure 5. N_2 adsorption–desorption isotherms of TS-1; (a) fresh, and (b) Spent.

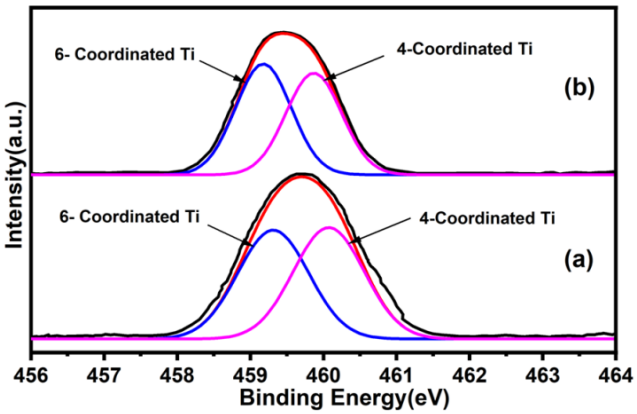

Figure 6. XPS spectra of TS-1 (Ti 2p): (a) fresh and (b) spent.

of nearby Si atoms silicate phase [43].

4 Catalytic Activities

Propylene to propylene oxide has been studied at different reaction conditions by using TS-1 catalyst in a batch reactor having 50mL capacity. The effect of temperature, pressure, reactant concentration has been discussed in details. The all experimental results are discussed with error of 5%.

4.1 Effect of Temperature and Pressure

The influence of total reaction pressure, with or without inert gas (Ar) on the catalyst activity was examined across a temperature range of 40–70°C (Figure 7(a) and 7(b)). Figures 7(a) present the effect of pressure with or without inert gas Ar on both the yield of propylene oxide, however Figure 7(b) represent the product selectivity. At 50°C the highest propylene oxide yields, around 2.33% and 2.28%, were observed at 10 bar and 5 bar of propylene without using Ar, respectively. The product yield decrease to 2.28 and 1.69% at 40°C under the same pressures. The product yield on adding of inert gas Ar in 1:1, 1:2 and 1:3 ratio of the reactant in the reaction system at 50 °C of reaction temperature are; 1.26 %, 2.13% and 1.08%, however the product distribution at reaction temperature of 40 °C are; 2.23 %, 1.91% and 1.64%, respectively. It is also observed that on increasing the temperature at any ratio of reactant to inert gas ratio, the product yield is going to decreases.

The product PO, selectivity at 50°C around 61.73% and 65.15%, were observed at 5 bar and 10 bar of propylene without using Ar, respectively. The product selectivity was 88.39% and 99.2% at 40°C under the same pressure condition (Figure 7(b)). The product selectivity on adding of inert gas Ar in 1:1, 1:2 and 1:3 ratio of the reactant in the reaction system at 50 °C of reaction temperature are; 98.7%, 54.56% and 99.25%, however the product selectivity at reaction temperature of 40 °C are; 57.5 %, 72.06% and 98.7%, respectively.

Overall, the system demonstrated excellent selectivity toward propylene oxide, reaching around 99.2% at 10 bar of propylene without inert gas and 40°C. Beyond this pressure range, no significant improvements in yield or selectivity were observed with or without inert gas. As the pressure approaches the liquefaction point of propylene (approximately 9.38 bar), changes in

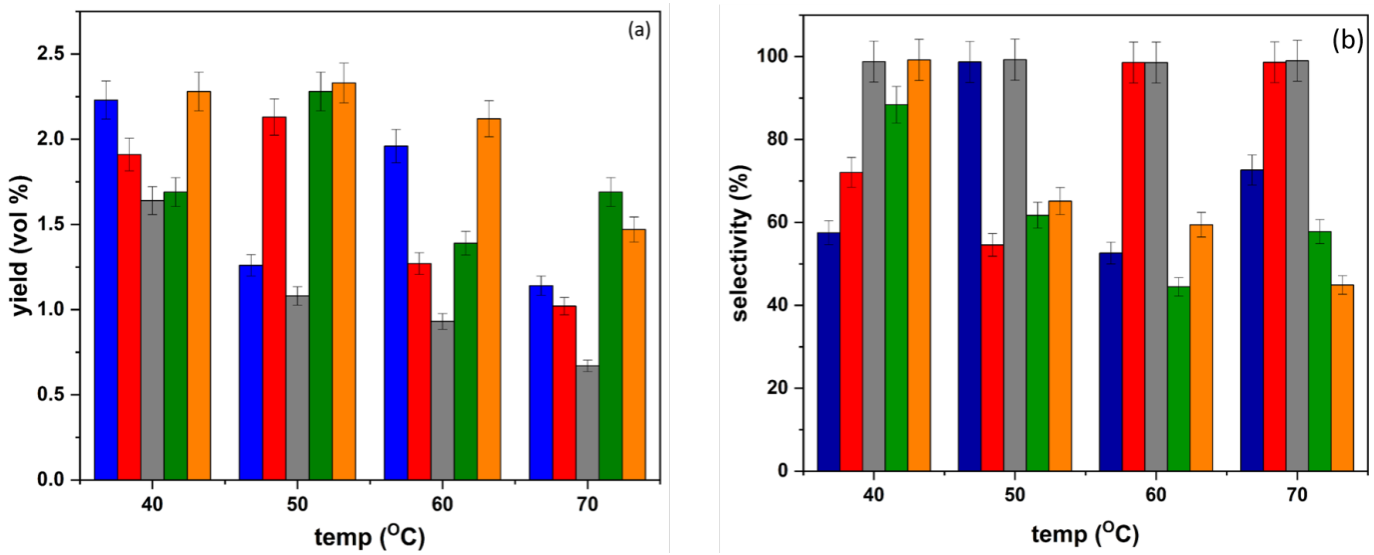

Figure 7. Effect of Inert gas, Ar over reaction temperature on PO yield (a) and selectivity (b) (Blue: 5 bar propylene and 5 bar Ar, Red: 5 bar propylene and 10 bar Ar, Gray: 5 bar propylene and 15 bar Ar, Green: 5 bar propylene and orange: 10 bar propylene).

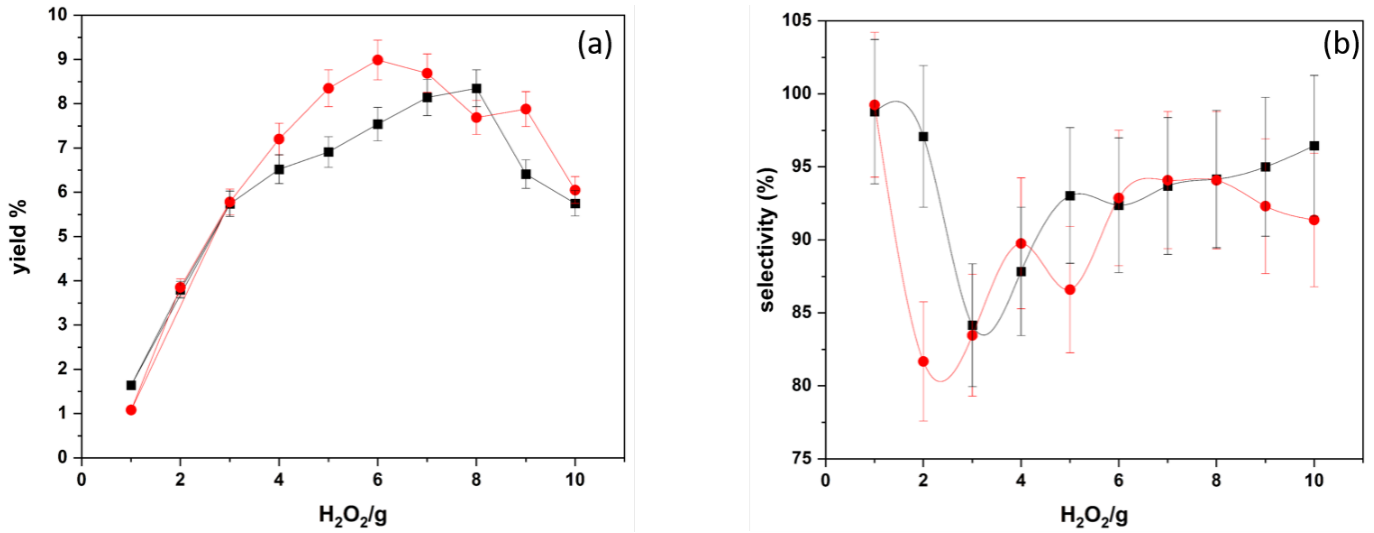

Figure 8. Effect of H_2O_2 on yield (a) and selectivity (b) of PO, at temp. 40°C (black) and at temp. 50°C (red).

propylene behavior may begin to influence the reaction. Notably, variations in pressure have only a slight effect on product selectivity, with differences of around 10% between the maximum (10 bar) and minimum (5 bar).

4.2 Effect of Hydrogen Peroxide Concentration under Different Temperatures

Hydrogen peroxide decomposition is closely linked to both the yield and selectivity of propylene oxide (PO). The influence of H_2O_2 concentration on propylene epoxidation is shown in Figure 8. A maximum PO yield of approximately 9% was obtained using 6.0 g of H_2O_2, and whereas the highest product selectivity of 99.5% was observed at a lower H_2O_2 amount of 2.0 g at a reaction temperature near 40 °C.

The breakdown of hydrogen peroxide is highly temperature-sensitive, showing an exponential increase with rising temperatures. Below 40°C the decomposition was minimal; however, at elevated temperatures, such as 50°C a noticeable reduction in the available H_2O_2 for reaction with propylene was detected.

The effect of hydrogen peroxide concentration was evaluated at 40 °C and a pressure of 5.0 bar. While increasing the H_2O_2 amount enhanced PO yield, it negatively impacted selectivity as discussed earlier. A distinct drop in PO selectivity was observed between 2 and 4 wt% H_2O_2, as illustrated in Figure 8(a) and 8(b). The reduction in selectivity could be attributed to the increased conversion of propylene,

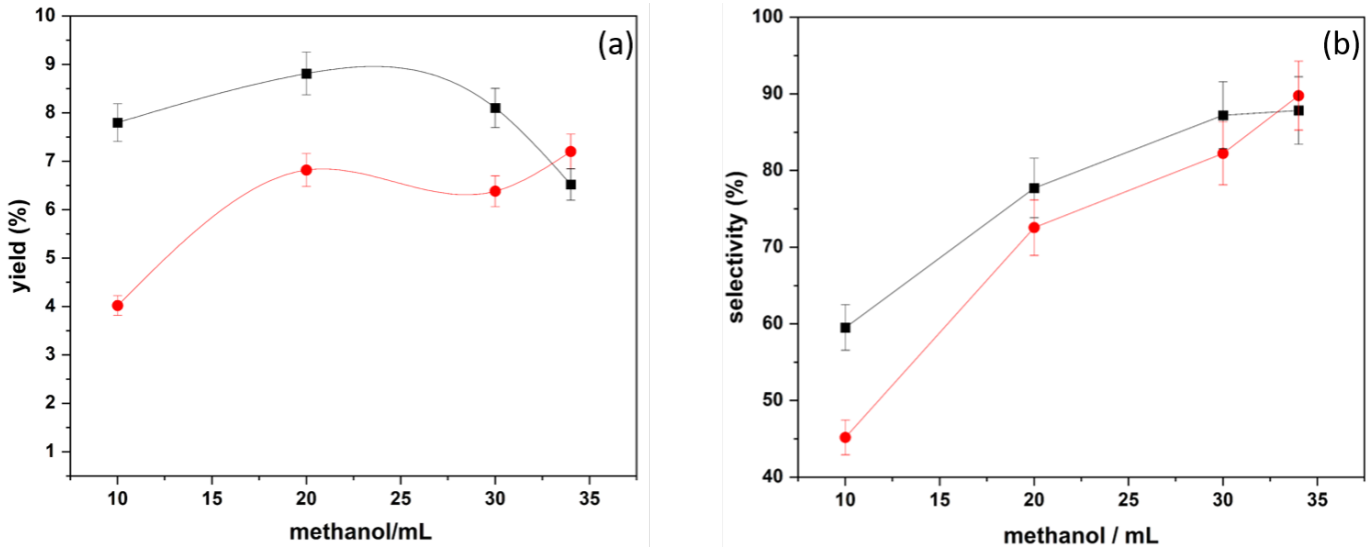

Figure 9. Effect of methanol on yield (a) and selectivity (b) of PO, at temp. 40°C (black) and at temp. 50°C (red).

which may promote side reactions, such as further transformation with methanol on the catalyst surface. These findings align with previously reported studies where reduction of selectivity was noticed with high hydrogen peroxide concentrations.6

4.3 Effect of Methanol under Different Temperatures

Methanol decomposition has a direct impact on both the yield and selectivity of propylene oxide (PO). The effect of methanol volume on the epoxidation of propylene is depicted in Figure 9. A peak PO yield of approximately 9% was obtained when 25 mL of methanol was used. However, the highest selectivity, around 90%, was observed with 35 mL of methanol at a relatively low reaction temperature of about 40°C.

The effect of methanol concentration was examined under reaction conditions of 40°C and 5.0 bar pressure. An increase in methanol volume enhanced the conversion of propylene-to-propylene oxide (PO), leading to improvements in both yield and selectivity. A significant rise in selectivity was particularly evident when the methanol volume increased from 30 - 35 mL, as illustrated in Figure 9(a) and 9(b).

On increasing the oxidizing agent (H_2O_2), propylene oxide yield (PO) increases and selectivity decreases (5% PO with 92% selectivity for 4 g of H_2O_2). As per the proposed reaction, 34 g of H_2O_2 is required to complete the oxidation of 42 g of C_3H_6. With the increase of the solvent, the PO yield and selectivity increase due to the dilution effect. The water may lead to hydrolysis of the main product, i.e., propylene oxide (PO), to propylene glycol (PG).

$$\underset{42.08\ \text{g}}{1\ C_3H_6} + \underset{34.0147\ \text{g}}{1\ H_2O_2} = \underset{58.080\ \text{g}}{1\ C_3H_6O} + \underset{18.0\ \text{g}}{1\ H_2O}$$

5 Conclusion

This study demonstrates the successful direct epoxidation of propylene to PO using a highly stable and efficient titanium silicate (TS-1) mesoporous catalyst. Comprehensive characterization confirmed the catalyst's high crystallinity, uniform particle morphology, and well-dispersed titanium sites, all of which are critical for catalytic performance. The TS-1 catalyst exhibited remarkable performance, achieving a maximum PO selectivity of 99.5% (at 2.0 g H2O2) and a maximum yield of 9% (at 6.0 g H2O2) under optimized temperature (40°C) and pressure (5 bar) conditions. Systematic variation of reaction parameters revealed that increasing hydrogen peroxide concentration enhances PO yield but can reduce selectivity due to side reactions, while higher methanol volumes improve both yield and selectivity by diluting reactants and minimizing byproduct formation. The catalyst also demonstrated robust stability and reusability, with minimal loss in activity after four cycles.

Data Availability Statement

Data will be made available on request.

Funding

This work was supported without any funding.

Conflicts of Interest

The authors declare no conflicts of interest.

Ethical Approval and Consent to Participate

Not applicable.

References

[1] Tullo, A. H., & Short, P. L. (2006). Propylene oxide routes take off. *Chemical & engineering news, 84*(41), 22-23. [CrossRef]

[2] Adiko, R. G. (2019). Pengaruh Current Ratio Dan Total Asset Turnover Terhadap Roa Pada Perusahaan Sektor Farmasi Yang Terdaftar Di Bei Priode 2009-2013. *Journal of Chemical Information and Modeling, 53*(9), 1689–1699. [CrossRef]

[3] Wexler, P., & Anderson, B. D. (Eds.). (2005). *Encyclopedia of toxicology* (Vol. 1). Academic Press.

[4] Anbarasu, M., Anandan, M., Chinnasamy, E., Gopinath, V., & Balamurugan, K. (2015). Synthesis and characterization of polyethylene glycol (PEG) coated Fe3O4 nanoparticles by chemical co-precipitation method for biomedical applications. *Spectrochimica Acta Part A: Molecular and Biomolecular Spectroscopy, 135*, 536-539. [CrossRef]

[5] Romano, U., & Ricci, M. (2013). Industrial applications. *Liquid phase oxidation via heterogeneous catalysis: organic synthesis and industrial applications*, 451-506. [CrossRef]

[6] Russo, V., Tesser, R., Santacesaria, E., & Di Serio, M. (2013). Chemical and technical aspects of propene oxide production via hydrogen peroxide (HPPO process). *Industrial & Engineering Chemistry Research, 52*(3), 1168-1178. [CrossRef]

[7] Chowdhury, B., Bravo-Suárez, J. J., Date, M., Tsubota, S., & Haruta, M. (2006). Trimethylamine as a gas-phase promoter: Highly efficient epoxidation of propylene over supported gold catalysts. *Angewandte Chemie International Edition, 45*(3), 412–415. [CrossRef]

[8] Ghosh, S., Acharyya, S. S., Tiwari, R., Sarkar, B., Singha, R. K., Pendem, C., ... & Bal, R. (2014). Selective oxidation of propylene to propylene oxide over silver-supported tungsten oxide nanostructure with molecular oxygen. *ACS catalysis, 4*(7), 2169-2174. [CrossRef]

[9] Serrano, D. P., van Grieken, R., Melero, J. A., & Garcia, A. (2004). Liquid phase rearrangement of long straight-chain epoxides over amorphous, mesostructured and zeolitic catalysts. *Applied Catalysis A: General, 269*(1-2), 137-146. [CrossRef]

[10] Virmani, A., Walavalkar, M. P., Sharma, A., Sengupta, S., Saha, A., & Kumar, A. (2020). Kinetic studies of the gas phase reaction of 1, 2-propylene oxide with the OH radical over a temperature range of 261–335 K. *Atmospheric Environment, 237*, 117709. [CrossRef]

[11] Sugiyama, S., Sakuwa, Y., Ogino, T., Sakamoto, N., Shimoda, N., Katoh, M., & Kimura, N. (2019). Gas-phase epoxidation of propylene to propylene oxide on a supported catalyst modified with various dopants. *Catalysts, 9*(8), 638. [CrossRef]

[12] Schmal, M. (2016). *Heterogeneous catalysis and its industrial applications*. Rio de Janeiro: Springer. [CrossRef]

[13] Pinna, F. (1998). Supported metal catalysts preparation. *Catalysis Today, 41*(1-3), 129-137. [CrossRef]

[14] Lu, M., Tang, Y., Chen, W., Ye, G., Qian, G., Duan, X., ... & Zhou, X. (2019). Explosion limits estimation and process optimization of direct propylene epoxidation with H2 and O2. *Chinese Journal of Chemical Engineering, 27*(12), 2968-2978. [CrossRef]

[15] Li, Z., Zhang, J., Wang, D., Ma, W., & Zhong, Q. (2017). Confirmation of gold active sites on titanium-silicalite-1-supported nano-gold catalysts for gas-phase epoxidation of propylene. *The Journal of Physical Chemistry C, 121*(45), 25215-25222. [CrossRef]

[16] Boronat, M., Pulido, A., Concepción, P., & Corma, A. (2014). Propene epoxidation with O 2 or H 2–O 2 mixtures over silver catalysts: theoretical insights into the role of the particle size. *Physical Chemistry Chemical Physics, 16*(48), 26600-26612. [CrossRef]

[17] Miyazaki, T., Ozturk, S., Onal, I., & Senkan, S. (2003). Selective oxidation of propylene to propylene oxide using combinatorial methodologies. *Catalysis Today, 81*(3), 473–484. [CrossRef]

[18] Li, G., Wang, X., Yan, H., Chen, Y., & Su, Q. (2001). Effect of sodium ions on propylene epoxidation catalyzed by titanium silicalite. *Applied Catalysis A: General, 218*(1-2), 31-38. [CrossRef]

[19] Deng, X., Wang, Y., Shen, L., Wu, H., Liu, Y., & He, M. (2013). Low-cost synthesis of titanium silicalite-1 (TS-1) with highly catalytic oxidation performance through a controlled hydrolysis process. *Industrial & Engineering Chemistry Research, 52*(3), 1190-1196. [CrossRef]

[20] Xiong, G., Hu, D., Guo, Z., Meng, Q., & Liu, L. (2018). An efficient Titanium silicalite-1 catalyst for propylene epoxidation synthesized by a combination of aerosol-assisted hydrothermal synthesis and recrystallization. *Microporous and Mesoporous Materials, 268*, 93-99. [CrossRef]

[21] Hertzsch, T., Hulliger, J., Weber, E., & Sozzani, P. (2013). Organic zeolites. In *Encyclopedia of Supramolecular Chemistry-Two-Volume Set (Print)* (pp. vol2-996). CRC Press.

[22] Chen, Q., & Beckman, E. J. (2008). One-pot green synthesis of propylene oxide using in situ generated hydrogen peroxide in carbon dioxide. *Green Chemistry, 10*(9), 934-938. [CrossRef]

[23] Sachtler, W. M., & Zhang, Z. (1993). Zeolite-supported transition metal catalysts. In *Advances in Catalysis* (Vol. 39, pp. 129-220). Academic Press. [CrossRef]

[24] Sinha, A. K., Seelan, S., Tsubota, S., & Haruta, M. (2004). Catalysis by gold nanoparticles: epoxidation of propene. *Topics in catalysis, 29*(3), 95-102. [CrossRef]

[25] Mccoy, M. (2001). New routes to propylene oxide. *Chemical & Engineering News, 79*(43), 19-19.

[26] Vaughan, O. P., Kyriakou, G., Macleod, N., Tikhov, M., & Lambert, R. M. (2005). Copper as a selective catalyst for the epoxidation of propene. *Journal of Catalysis, 236*(2), 401-404. [CrossRef]

[27] Yap, N., Andres, R. P., & Delgass, W. N. (2004). Reactivity and stability of Au in and on TS-1 for epoxidation of propylene with H2 and O2. *Journal of Catalysis, 226*(1), 156-170. [CrossRef]

[28] Qi, C., Okumura, M., Akita, T., & Haruta, M. (2004). Vapor-phase epoxidation of propylene using H2/O2 mixture over gold catalysts supported on non-porous and mesoporous titania-silica: Effect of preparation conditions and pretreatments prior to reaction. *Applied Catalysis A: General, 263*(1), 19-26. [CrossRef]

[29] Haruta, M., & Daté, M. (2001). Advances in the catalysis of Au nanoparticles. *Applied Catalysis A: General, 222*(1-2), 427-437. [CrossRef]

[30] Clerici, M. G., Bellussi, G., & Romano, U. (1991). Synthesis of Propylene Oxide from Propylene and Hydrogen Peroxide Catalyzed by Titanium Silicalite. *Journal of Catalysis, 129*(1), 159–167. [CrossRef]

[31] Huang, M., Wen, Y., Wei, H., Zong, L., Gao, X., Wu, K., Wang, X., & Liu, M. (2021). The Clean Synthesis of Small-Particle TS-1 with High-Content Framework Ti by Using NH4HCO3 and Suspended Seeds as an Assistant. *ACS Omega, 6*(20), 13015–13023. [CrossRef]

[32] Khouchaf, L., Boulahya, K., Das, P. P., Nicolopoulos, S., Kis, V. K., & Lábár, J. L. (2020). Study of the microstructure of amorphous silica nanostructures using high-resolution electron microscopy, electron energy loss spectroscopy, X-ray powder diffraction, and electron pair distribution function. *Materials, 13*(19), 4393. [CrossRef]

[33] Owens, G. J., Singh, R. K., Foroutan, F., Alqaysi, M., Han, C.-M., Mahapatra, C., Kim, H.-W., & Knowles, J. C. (2016). Sol–gel based materials for biomedical applications. *Progress in Materials Science, 77*, 1–79. [CrossRef]

[34] Yang, J., Liu, S., Liu, Y., Zhou, L., Wen, H., Wei, H., Shen, R., Wu, X., Jiang, J., & Li, B. (2024). Review and Perspectives on TS-1 Catalyzed Propylene Epoxidation Science. *Science, 27*(3), 109064. [CrossRef]

[35] Inkson, B. J. (2016). Scanning electron microscopy (SEM) and transmission electron microscopy (TEM) for materials characterization. In *Materials Characterization Using Nondestructive Evaluation (NDE) Methods* (pp. 17–43). [CrossRef]

[36] Teamsinsungvon, A., Ruksakulpiwat, C., Amonpattaratkit, P., & Ruksakulpiwat, Y. (2022). Structural Characterization of Titanium–Silica Oxide Using Synchrotron Radiation X-Ray Absorption Spectroscopy. *Polymers, 14*(13), 2729. [CrossRef]

[37] Guan, Z. L., Wang, Y. D., Wang, Z., Hong, Y., Liu, S. L., Luo, H. W., ... & Su, B. L. (2024). The synthesis, characteristics, and application of hierarchical porous materials in carbon dioxide reduction reactions. *Catalysts, 14*(12), 936. [CrossRef]

[38] Tanev, P. T., & Pinnavaia, T. J. (1996). Biomimetic templating of porous lamellar silicas by vesicular surfactant assemblies. *Science, 271*(5253), 1267-1269. [CrossRef]

[39] Guo, Y., Zhou, L., Guo, F., Chen, X., Wu, J., & Zhang, Y. (2020). Pore Structure and Fractal Characteristic Analysis of Gasification-Coke Prepared at Different High-Temperature Residence Times. *ACS Omega, 5*(35), 22226–22237. [CrossRef]

[40] Bhaumik, A., Samanta, S., & Mal, N. K. (2004). Highly active disordered extra large pore titanium silicate. *Microporous and Mesoporous Materials, 68*(1–3), 29–35. [CrossRef]

[41] Wang, Q., Wang, L., Chen, J., Wu, Y., & Mi, Z. (2007). Deactivation and regeneration of titanium silicalite catalyst for epoxidation of propylene. *Journal of Molecular Catalysis A: Chemical, 273*(1-2), 73-80. [CrossRef]

[42] Chinh, V. D., Broggi, A., Di Palma, L., Scarsella, M., Speranza, G., Vilardi, G., & Thang, P. N. (2017). XPS Spectra Analysis of Ti2+, Ti3+ Ions and Dye Photodegradation Evaluation of Titania-Silica Mixed Oxide Nanoparticles. *Journal of Electronic Materials, 47*(4), 2215–2224. [CrossRef]

[43] Brassard, D., & Khakani, M. A. E. (2007). Substrate biasing effect on the electrical properties of magnetron-sputtered high-k titanium silicate thin films. *Journal of Applied Physics, 102*(3), 034106. [CrossRef]